



Can field data constrain rock viscosities?

C.J. Talbot

Hans Ramberg Tectonic Laboratory, Department of Earth Sciences, Uppsala University, 752 36 Uppsala, Sweden

Received 15 April 1998; accepted 23 December 1998

Abstract

In the 1960s it looked as though the ratio of wavelength to thickness of folds along shortened competent single layers might allow constraint of the viscosity ratios between the layers and their hosts when they deformed together. In the 1970s, the possibility arose that simple field measurements of boudins and mullions might also constrain rock viscosity ratios and thereby distinguish deformation facies and map rock viscosities in pressure–temperature–time space. Even more potential tools for constraining rock viscosities appeared in the 1980s but since then progress appears to have stagnated in a welter of problems.

An attempt is made to refocus attention on direct retrospective measurements of rock rheologies during natural deformations by reviewing the potential field tools for constraining rock viscosities, discussing some of their problems, and by a crude application of the most developed approach. Further advances are likely to come from iteration between modellers and structural geologists working in a variety of tectonic settings. As well as constraining the pressure–temperature–time paths of our rocks, we should also be attempting to measure their viscosities. © 1999 Elsevier Science Ltd. All rights reserved.

1. Introduction

One of the weakest aspects of current structural geology is our ignorance concerning rock rheologies and the rates of deformation processes in different tectonic environments. The statements of Pfiffner and Ramsay (1982) that typical axial ratios of strain between 1 and 10 in young orogens imply rates of strain between 10^{-13} s^{-1} and 10^{-15} s^{-1} , and that differences in strain rate seldom exceed 10, have not been improved significantly. Modellers currently use generic viscosity contrasts, or laboratory measurements extrapolated over several orders of magnitude in time. The common practice of assigning a single viscosity to the whole of the lower continental crust may be appropriate for modelling large-scale tectonic processes but is inappropriate for modelling processes on scales less than about 1 km in which gravity plays a relatively insignificant role. Asking whether the viscosities of individual rock types could be constrained using simple field measurements leads to a review of the potential tools,

an outline of their obvious problems, and a crude demonstration of their potential in an attempt to kick-start a new round of discussion of what is already an old chestnut of a problem. The basic problem is that shared by strain analysis, much has been published about the tools but not enough about the results of their application.

Most structural geologists are familiar with the use of the geometries of such sedimentary bedforms as ripples and dunes to distinguish sedimentary facies in plots of clastic grain size against flow velocity, stream power, or shear stress (Pye, 1994). Similarly, many of us have used the chemistries of stable mineral assemblages calibrated in a range of experimental conditions to constrain the pressure–temperature–time (P – T – t) paths followed by particular rocks through metamorphic facies distinguished in P – T space. But how many of us have considered using simple relationships between structures or fabrics to track rock rheologies through deformation facies distinguished in P – T space? Deformation facies could be defined by relative ductilities, and viscosity ratios in the ductile domain could potentially be constrained by field measurements limited by laboratory measurements of viscosities.

E-mail address: christopher.talbot@geo.uu.se (C.J. Talbot)

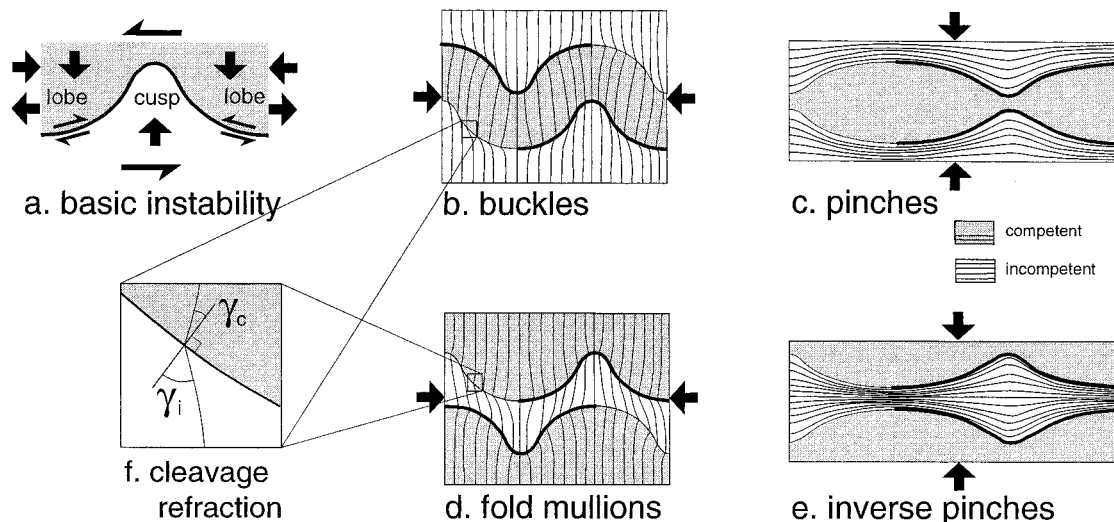


Fig. 1. Structures and fabric relationships discussed here for measuring the viscosity ratio of adjoining competent (dark) and less competent (clear) ductile materials. (a) The basic shear instability of incompetent cusps alternating with competent lobes along strain-active interfaces can be driven by a wide range of forces (as indicated by an incomplete suite of arrows). Cusps and lobes along the contacts of thin single layers interfere to produce four categories of structures (b–e) that depend on the sign of the μ_h/μ_l ratio and the direction of shortening. Cusps are antisymmetric across layers shortened along their length (b, d) and symmetric along layers shortened across their length (c, e). (f) The angles used to measure viscosity ratios by cleavage refraction.

Mineralogists began distinguishing metamorphic facies by focusing on only a limited suite of minerals and rocks (e.g. polymorphs of Al_2SiO_5 and pelites). Similarly, deformation facies might be distinguished by focusing on only a few rock pairs. Such an approach is advocated here and illustrated in rudimentary form for the purpose of discussion and improvement.

2. Approach

2.1. Refining the brittle–ductile transition

The nearest structural geologists come to recognising deformation facies at the moment is the general distinction of an upper crustal domain in which most rock masses strain along brittle fractures from a lower crustal domain in which most rocks flow. However, many field geologists have seen tabular boudins of one rock type initially separated along fractures in another that flowed—but how many of us refine the brittle–ductile transition boundary by accumulating such observations on P – T plots constrained by metamorphic mineralogy? Our understanding of rock rheologies could be improved by such simple observations.

2.2. Deformation facies in the ductile domain

The basic tools for the qualitative distinction of deformation facies within the ductile domain are the different geometries displayed by deformation structures developed along strain-active interfaces and by

fabrics developed across such contacts (see also Treagus, this issue, who also deals with inclusions). Relative competence comes from the fundamental shear instability in which cusps of incompetent material alternate with lobes of a more competent material along deformed strain-active interfaces (Fig. 1a, after Ramsay, 1967). The direction of refraction of any contemporaneous cleavage should confirm the relative competence indicated by cusps, for, as discussed in more detail by Treagus (this volume), cleavage refracts towards strain-active interfaces in less competent layers and away from them in adjoining more competent layers (inset on Fig. 1, after Treagus, 1983).

The relative competence of granitoid and basaltic rock types changes qualitatively in the ductile field. Other rock pairs may change relative competence over limited P – T conditions but the swap between granitoid and basaltic rocks will be used here to illustrate their potential for defining deformation facies.

Consider the deformation of basaltic sheets intruded into granite. Where deformed at low temperatures, cusps along mafic sheets point inward and indicate that the mafic sheets deformed more slowly than the surrounding granite and either buckled or pinched depending on their orientation. However, where deformed together at higher temperature, cusps along mafic sheets instead point outward between inward bulging lobes of more competent granite (Talbot and Sokoutis, 1992). The mineralogies of the mafic layers differ but their chemistries are essentially similar and the relative strain rates of this rock pair have interchanged at some intermediate temperature. When

pinned down, this swap will distinguish a ‘basalt-competent-in-granite’ deformation facies from another ‘basalt-incompetent-in-granite’ facies. Talbot and Sokoutis (1992) describe a case where this boundary in deformation facies migrated in space between two separable phases of deformation, from where a ‘second’ deformation mullioned ‘first’ generation boudins of mafic sheets in a granitic gneiss to where the second deformation remullioned first generation mullions in mafic sheets of the same suite a few hundred metres away.

3. Tools for constraining viscosity ratios in the ductile domain

Quantitative subdivisions within deformation facies are potentially possible by constraining viscosity ratios for common rock pairs using two tools already available and other potential tools that need further development. Examples of deformed single layers of essentially similar chemistry that are common in other rocks with a wide range of chemistries in many tectonic environments are veins of quartz or calcite and intrusive sheets of basaltic or granitoid rocks.

3.1. Cleavage refraction angle

Consider

$$\mu_c/\mu_i = \gamma_i/\gamma_c \quad (1)$$

the equation, first developed by Treagus (1983, 1988) and demonstrated experimentally by Treagus and Sokoutis (1992), which relates the finite shear γ resulting from cleavage refraction in competent (subscript c) and incompetent (subscript i) materials to the ratio of their effective viscosities, μ (see Fig. 1f). Treagus discusses the potential and limitations of this, the simplest tool for measuring the ratios of linear or non-linear viscosities for rock pairs, in more detail (this issue) and reports the first results of its application. Viscosity ratios derived independently from cleavage refraction angles and cusp wavelengths (see below) in particular rock pairs would obviously provide useful cross checks.

3.2. Ratios of wavelength to thickness of buckled competent single layers

In a series of ten papers between 1957 and 1963, Biot and Ramberg (reviewed in Fletcher, 1977) were the first to apply the theory of thin sheet approximation to relate the ratio of dominant wavelength to the thickness (L_d/t) of buckled competent layers to the ratio of the viscosity of the layer to its host rock

(μ_l/μ_h). Biot (1961) showed

$$L_d = 2\pi t \left(\frac{\mu_l}{6\mu_h} \right)^{1/3} \quad (2)$$

However, this solution predicts folds with $L_d/t = 6$ even in strain-inactive markers ($\mu_l/\mu_h \approx 1$) and fails to predict the short wavelengths (between four and six times the thickness) common in natural populations of fold trains (Smith, 1977). Biot’s solution for thin sheets was generalised to thick layers of non-linear layers (Fletcher, 1974) and Newtonian layers (Fletcher, 1977; Smith, 1977) but, these solutions still applied only to buckles in thin layers shortened up to a few per cent, whereas many natural folds are shortened much more. Hudleston (1973) took account of the homogeneous component of finite shortening by inserting the square root of the ratio of principal quadratic elongations, $S = (\lambda_1/\lambda_2)^{-1/2}$ in the far-field of the host rocks. In the relevant profile, we can recover the viscosity ratio from the ratio of the finite dominant wavelength, L_d , and thickness, t , of single layers cylindrically buckled by finite shortening:

$$L_d = 2\pi t \left\{ \left(\frac{\mu_l}{6\mu_h} \right) \times \frac{1}{2} \left(S + \frac{1}{S^2} \right) \right\}^{1/3} \quad (3)$$

However, natural populations of cylindrical folds in single layers seldom display regular periodic waveforms (Sherwin and Chapple, 1968; Hudleston, 1973). A method was needed to identify the dominant wavelength among the complex inflections that develop in natural populations of folds in single layers. Fletcher and Sherwin (1978) argued that measuring fold arc lengths L along the mid-plane of the layer of finite amplitude folds recovers the wavelength at the end of the selection phase when the fold hinges begin to thicken and the limbs begin to thin. Fletcher and Sherwin (1978) then checked a theory for wavelength selection developed earlier (Sherwin and Chapple, 1968). This takes account of the uniform thickening and shortening during folding and outlines a comparatively simple method for deriving viscosity ratios from folded single layers.

Fletcher and Sherwin (1978) advocated measuring fold arc length, L , which is twice the distance measured along the mid-line of the layer between successive hinges measured in units of t , the layer thickness. L has a frequency distribution, $f(L)$ with a single well-defined maximum. Then δ , the dispersion of $f(L)$, is used as a measure of the regularity of folding

$$\delta = \sigma/\underline{L} \quad (4)$$

where σ is the standard deviation of $f(L)$ and \underline{L} is the mean value of L .

The dominant wavelength L_d is then found using \underline{L}

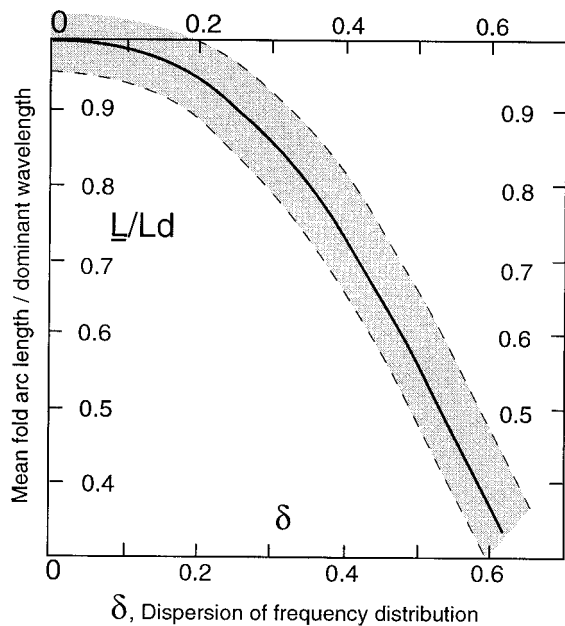


Fig. 2. Ratio of mean fold arc length \underline{L} to dominant wavelength L_d (\underline{L}/L_d) plotted against the dispersion of its frequency distribution $\delta = \sigma/\underline{L}$. The solid curve is a free-hand fit to data produced by over 200 numerical simulations by Fourier synthesis of low limb-dip fold trains with a uniform simple amplitude spectra (skewed to longer wavelength) with a range of bandwidths. The dashed curves indicate the scatter likely in measurements of the parameters plotted from a folded single layer of length $50L_d$. (Simplified from fig. 5 of Fletcher and Sherwin, 1978.)

and δ in Fig. 2 (a simplification of fig. 5 in Fletcher and Sherwin, 1978). The viscosity ratio is then found by inserting L_d/t in Fig. 3 (a simplification of fig. 3 in Fletcher, 1977) which produces results not very different from applying expression (2) by Biot (1961). Having developed a practical tool for constraining rock viscosities from natural folds, Fletcher and Sherwin (1978) pointed to the potential of knowing from experiments the rheology of one of the rock pair analysed, a theme developed further here.

Chapple (1970) reviewed 20 years of development in the recovery of rheological ratios from competent single layers that display buckles with low or high amplitude and may have buckled as linear elastic, viscoelastic, Newtonian or non-linear viscous materials.

3.3. Other potential tools

In an exciting development, Smith generalised the theory of how viscosity ratios relate to ratios of initial wavelengths to thickness of single layers for all four potential combinations (Fig. 1b–e) of the fundamental shear instability (Fig. 1a), first in Newtonian fluids (1975) and then in non-linear fluids (1977). Suddenly, there was the possibility that viscosity ratios might come, not only from folds, but also from flow boudins and what Smith unfortunately called inverse folds and

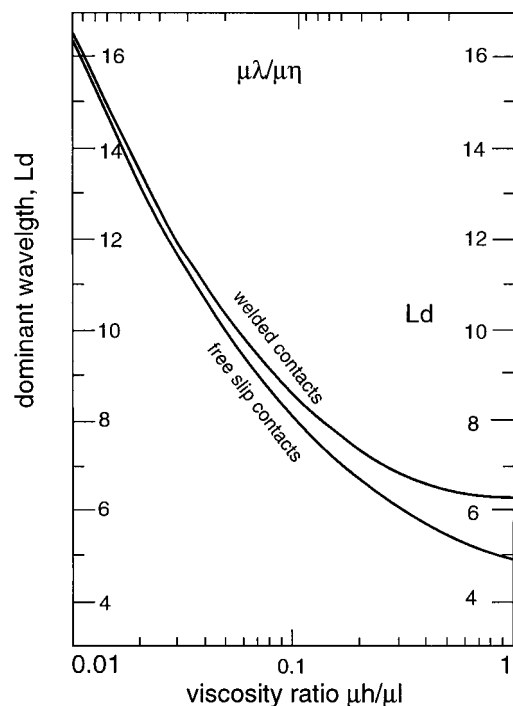


Fig. 3. Dominant wavelengths of single layers with welded and free slip contacts plotted against the ratio of the viscosity of the layer to the host (simplified from fig. 3 in Fletcher, 1977). Fletcher showed:

$$q(k;R) = -2(1-R)\{(1-R^2) - [(1+R)^2 e^k - (1-R)^2 e^{-k}]/2k\}^{-1} \quad \text{for non-slip}$$

$$q(k;R) = -2\{1 - [(e^k - e^{-k}) + R(e^k + e^{-k})]/2k\}^{-1} \quad \text{for free slip}$$

where $k = 2Lt$ and $R = \mu_h/\mu_l$, and q is a measure of the rate of amplification of a fold component with the instantaneous value of the dimensionless wavenumber k . The wavenumber of the component which is amplified at the greatest instantaneous rate, k_d , maximises q . The quantity $L_d = (2\pi/k_d)t$ is the dominant wavelength (Biot, 1961).

inverse boudins. Introducing the non-linear factor of strain rate softening increased the growth rate of all four instabilities, but to different degrees. Non-linear flow was shown to fit observations better than Newtonian flow by relating the likelihood of a type of structure to the strength of the instability responsible for it. Buckles (Fig. 1b) are the most common structures because they are generated by the strongest instability, flow boudins (Fig. 1c) are common because of a strong instability, what Smith called *inverse boudins* are uncommon because of a relatively weak instability and what he called *inverse folds* are the rarest because this instability is weakest (Smith, 1977).

Smith (1977) called the structures along shortened incompetent layers *inverse boudins* because he considered them to be symmetric across the midplane of the layer (as in pinches, Fig. 1c). He labelled outward pointing cusps along extended incompetent layers *inverse folds* because he took them to be antisymmetrical across the midplane (as in buckles, Fig. 1b).

However, both field observations (Talbot, 1983; Talbot and Sokoutis, 1995) and experiments (Sokoutis, 1987, 1990) indicate that the actual symmetries are the opposite (definitely for fold mullions, less certainly for inverse boudins) and that Smith's terms should be reversed. Thus outward pointing cusps along incompetent layers shortened along their length are antisymmetric and, where the wavelength is longer than the layer thickness, develop as what Ramsay (1967) called class 3 (divergent isogon) folds with an axial planar cleavage. These could be called inverse folds but will here be called *fold mullions* (Fig. 1d). Notice that fold mullions must develop in the incompetent host rock alongside buckles. Similarly, the outward pointing cusps (with contact-parallel cleavage) that are rare along extended incompetent single layers are ubiquitous alongside pinches between flow boudins (Fig. 1e) so that *inverse pinches* is a more appropriate label (Talbot and Sokoutis, 1992).

The original confusion may have arisen because Smith (1975) started his analysis by assuming that the strain rate of the more competent material controls the development of all four fundamental shear instabilities. However, the stresses that deform single layers are transmitted from their host rocks. It is therefore, arguable that structures develop along their contacts to allow single layers to conform to the rate of bulk pure shear of their host rocks. In these terms, the antisymmetric pinches that interfere to generate buckles can be considered as accelerating the shortening of competent single layers to keep pace with the bulk rate of shortening of their incompetent country rocks. Similarly, the instabilities that develop in the contacts of extending competent layers interfere to generate flow boudins that localise extension to regular symmetrical *pinches* (Fig. 1c) so that the competent layers can extend as fast as their incompetent host rock. Conversely, fold mullions slow the shortening of incompetent single layers to the bulk shortening rate of their competent host rock, just as outward pointing cusps slow the extension rate of incompetent layers.

This logic breaks the symmetry of Smith's argument (Smith, 1975, 1977) that dynamic and kinematic growth co-operate in amplifying perturbations during layer parallel shortening but compete during extension of single layers. Smith's argument led him to consider that buckles and boudins initiate with equal wavelengths, and that what I call here *fold mullions* (Fig. 1d) and *inverse pinches* (Fig. 1e) start with wavelengths that equal each other but differ from the initial wavelength shared by buckles and boudins. However, while buckles develop in a shortened competent layer, mullions develop simultaneously in the host rocks on either side. Similarly, pinches and inverse pinches develop simultaneously on either side of shared elongated contacts. Interference between cusps and

lobes developing on either side of deformed single layers may be controlled by the strain rate of the competent material whether they have shortened or extended. However, it is clear that wavelengths are shared, not by structures developing along single layers of particular competence, but by shortened or extended single layers whatever their competence. Rephrasing Smith (1977): dynamic secondary flow and kinematic pure shear co-operate to accelerate the rock with higher viscosity and compete to retard the rock with lower viscosity during the development of all four instabilities. Fold mullions and inverse pinches are uncommon and rare along single incompetent layers but as common as folds and pinches in the host rocks along the outer contacts of shortened and extended competent layers. Similarly, folds and pinches are common along single competent layers but as infrequent as fold mullions and inverse pinches in the host rock along the outer contacts of shortened and extended incompetent layers.

Subsequently, Smith himself (Smith, 1979) complicated the constraint of viscosity ratios from folded layers when he pointed out that the data set for natural fold populations displayed a suspicious tendency to cluster around folds with short wavelengths (i.e. L_d/t between 4 and 6). As an explanation, Smith suggested that shortwave folding of competent layers involved a new effect in host rocks that are strongly non-Newtonian. He showed how the secondary flow associated with one active interface deforms other interfaces, particularly those near $L_d/t = 4$ away; resonance between instabilities on interfaces with this spacing amplify each other. Unfortunately, this resonance is entirely geometric and thus insensitive to the viscosity contrast in host rocks deforming with large effective viscosities. Following his own logic, Smith (1979) assumed that shortwave resonance would apply equally to boudins whereas I would anticipate that it applies to mullions. Care must, therefore, be taken using both shortwave folds (and fold mullions?) to constrain viscosity contrasts.

Sokoutis (1990) raised another complication when he showed that increased shortening along incompetent layers can lead to kinematic pure shear squeezing incompetent materials out of cusps. This process deactivates increasing numbers of fold mullions that are left as horns or flames at the distal end of decreasing numbers of still-active fold mullions. The horns and flames of incompetent rock that are often visible in the cores of mature buckles therefore casts doubt on earlier assumptions that folds in competent layers merely tighten and that initial wavelengths are still recognisable after finite shortening. The wavelengths of fold mullions (and therefore of 'half folds' on the other side of a mutual contact) can apparently decrease by indi-

vidual instabilities deactivating during large shortenings.

Another tool with potential for limiting viscosity ratios might be the critical thicknesses at which single layer extension is stable or unstable (Talbot, 1970; Talbot and Sokoutis, 1992). Talbot (1970) used theory by Sokolovski (1945) to rationalise his finding that it is common for planar but obviously extended quartz veins to parallel quartz veins pinched during the same homogeneous bulk strain of the same host rock. Vein thickness was more pertinent than their orientation: thick veins pinched while thin veins extended uniformly during the same deformation. Above the critical thickness, extension of competent single layers is unstable so that they pinch; below the critical thickness, extension of layers with the same composition and orientation is stable so that irregularities are drawn out and they extend uniformly. The critical thickness of extended single layers can be expected to depend on the viscosity ratio between the layers and their host and thus differ with P – T conditions.

Treagus (this issue) suggests that cleavage refraction should be capable of mapping differences in the ratios of effective viscosities of non-linear fluids as past stresses changed around a particular fold in a single contact. By comparison, the ratios of wavelength to thickness of structures developed along single layers give averages of the ratios of viscosities effective along the whole layer. Recognising differences in effective viscosity ratios due to different stress histories would require relating variations in the wavelength/thickness ratio of structures in a population of layers to the orientation of each layer within the relevant strain ellipsoid (Talbot, 1970; Talbot and Sokoutis, 1992).

More work is obviously needed before viscosity ratios can routinely be constrained by field measurements of flow boudinage, fold mullions or inverse pinches. Can you think of any new approaches to paleoviscometry?

4. Application

Viscosity ratios derived using developments of the approaches outlined above could be plotted in various co-ordinates. Perhaps, the first should always be simple plots of the relationship in the governing expression to check that the data are consistent. Because the viscosities of rocks are almost certainly non-linear with temperature, consistent data could then be transferred to a plot of log strain rate (s^{-1}) against temperature ($T^{\circ}C$) or, more useful for modellers, logarithmic equivalent stress. Alternative co-ordinates include (for comparison with maps of deformation mechanisms used by rock mechanics), logarithmic viscosity plotted against homologous temperature in

Table 1

Rock layer	Met. grade or $T^{\circ}C$	Location	Thickness range in population	n of L^a	\underline{L} mean fold arc length	$\sigma = \text{standard deviation of } \underline{L}$	dispersion, $\delta = \sigma/\underline{L}$	L_d	$\mu_{\text{layer}}/\mu_{\text{host}}$
<i>quartz vein</i>	Slate+amorph. C	Luing, Scotland	1–8 mm	66	4.48	2.52	0.56	10.4	20
black slate	< 150°C								
<i>basalt sheet</i>	Slate+amorph. C	Luing, Scotland	20–50 cm	8	6.43	2.54	0.395	8.93	11
black slate	< 150°C								
<i>quartz vein</i>	amphibolite ky + sill	Chimanda, Zimbabwe	5–17 cm	26	5.03	3.80	0.76	50.3	c. 10 000
pelite gneiss	c. 720°C							by extrapolation	by extrapolation
<i>basalt sheet</i>	amphibolite ky + sill	Chimanda, Zimbabwe	13–38 cm	16	4.52	1.75	0.389	6.19	8 (free)
pelite gneiss	c. 720°C								1 (welded)
<i>quartz vein</i>	c. 600°C	Trondheim, Norway	3.5–8.5 cm	58	3.25	1.68	0.052	6.5	7
pelite gneiss									
<i>quartz vein</i>	c. 600°C	Rat Rapids, Ontario	15–38 mm	11	4.52	1.55	0.34	5.65	5 (slip)
granite									

^a L = the fold arc length is twice the distance between successive fold hinges along mid-line of cylindrical folds measured in units of layer thickness. Then $\delta = \sigma/L$ where δ is a measure of the regularity of folding given by the dispersion of $f(L)$, σ is the standard deviation of $f(L)$ and \underline{L} is the mean value of L . Measure L , find \underline{L} and δ , and use them to find the dominant wavelength from Fig. 2 (or fig. 5 in Fletcher and Sherwin, 1978). Then use L_d in Fig. 3 (or fig. 3 in Fletcher, 1977) to find the viscosity contrast.

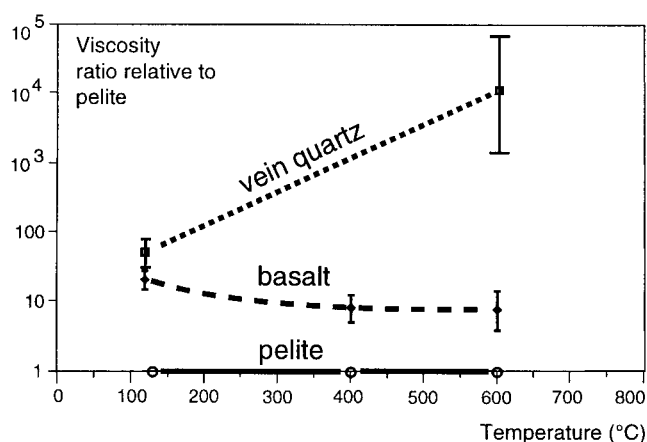


Fig. 4. The viscosities for quartz veins and basalt layers related to pelite with a fixed viscosity with $T^{\circ}\text{C}$ (data from Table 1) indicate that rock viscosities change with $T^{\circ}\text{C}$.

Kelvin (the ratio between the melting point of the rock in K and the temperature of deformation in K). However, it is arguable that strain rates (Price, 1975) are too vulnerable to the choice of spatial reference frame for routine practice. As a result, plots of logarithmic viscosity (μ in Pa s) against coeval metamorphic grade or temperature ($T^{\circ}\text{C}$) are considered most direct and practical here.

Table 1 lists some data derived by applying the approach suggested by Fletcher and Sherwin (1978) to some of my own field data or photographs and incomplete gleanings from the literature (see also Treagus, this issue). The categories 'pelite', 'basalt' or 'granite' are taken to denote bulk rock chemistries independent of mineralogy. Plotted as simple ratios relative to pelite (arbitrarily taken as having a constant viscosity for purely illustrative purposes), even so few data demonstrate the obvious, that the viscosity of basaltic rocks changes with temperature (Fig. 4).

Conversion of viscosity ratios derived from field data (cf. Fig. 4) into absolute viscosity ranges requires calibration against laboratory measurements. Figure 5 is a crude, poorly constrained indication of the viscosity ranges of some metamorphic and igneous rocks plotted in μ/T space presented as a challenge for others to improve. Boundaries on Fig. 5 are shown solid where they are constrained by experimental data, dashed where they are constrained by field data, and dotted where they have been interpolated or extrapolated. The field data (Fig. 4) have been related (Fig. 5) mainly to the viscosities of 'granites' (some via basalts) which are comparatively well known (Cruden, 1990) and can be extrapolated to the extraordinary 20 y measurements at room temperature reported by Ito (1979). Like all experimental work, Ito's is plagued by

the possibility that the creep rate he measured had not yet steadied. It did not specify the water content of his specimens but it is reasonably obvious by extrapolation of data from other experiments that they were rather wet. Future work should take account of as many as possible viscosities constrained for other rock types by long term experiments.

5. Discussion

The largest viscosity contrast on Table 1, of four orders of magnitude ± 1 order (averaged from 26 field readings), is exceeded at the same $T^{\circ}\text{C}$ by laboratory measurements of the viscosities of granitoid rocks with different water contents (Fig. 5). Unlike laboratory experiments no direct relationship can be assumed between field measurements of viscosity contrast and stress difference even in linear Newtonian fluids because deformation structures develop to equilibrate the driving stresses. Notice on (Fig. 5) that quartz veins exhibiting fold mullions in basaltic rocks would distinguish another rheological facies boundary.

The almost complete cross-over in relative competence between silicic melts and glasses that are more competent than basaltic melts and glasses to crystallising basalts that are more competent than most crystallising granites (between 1200 and 700°C on Fig. 5) probably accounts for the local structural complications seen in magma mixing and mingling. The overlap in the fields indicating the viscosities of wet ductile basaltic rocks and dry ductile granitic rocks (Fig. 5) accounts for most basaltic sheets shortened in granites being mullioned at amphibolite facies and folded at lower metamorphic grades. The entirely different mineralogies of 'basaltic rocks' at different metamorphic grades is an obvious explanation for their different viscosities, (the chemistries but not mineralogies of pelites and granites can also be similar) but we need values for viscosities.

Viscosities of rock can be anisotropic and depend on such factors as applied stress differences, confining pressure, fluid pressure, grain size and mineralogy as well as temperature and chemistry, so there are many more complications on the way to mapping rock viscosities in natural environments than space allows discussion of here.

The basic tools for defining and refining deformation facies have been around for the same three or four decades as those used to constrain P - T - t paths through well defined metamorphic facies. So why are the histories of rock viscosities not yet routinely reconstructed through P - T space? Perhaps those working with ductile strains have found it adequate to work with metamorphic P - T - t paths. Perhaps the link between metamorphism and deformation has been

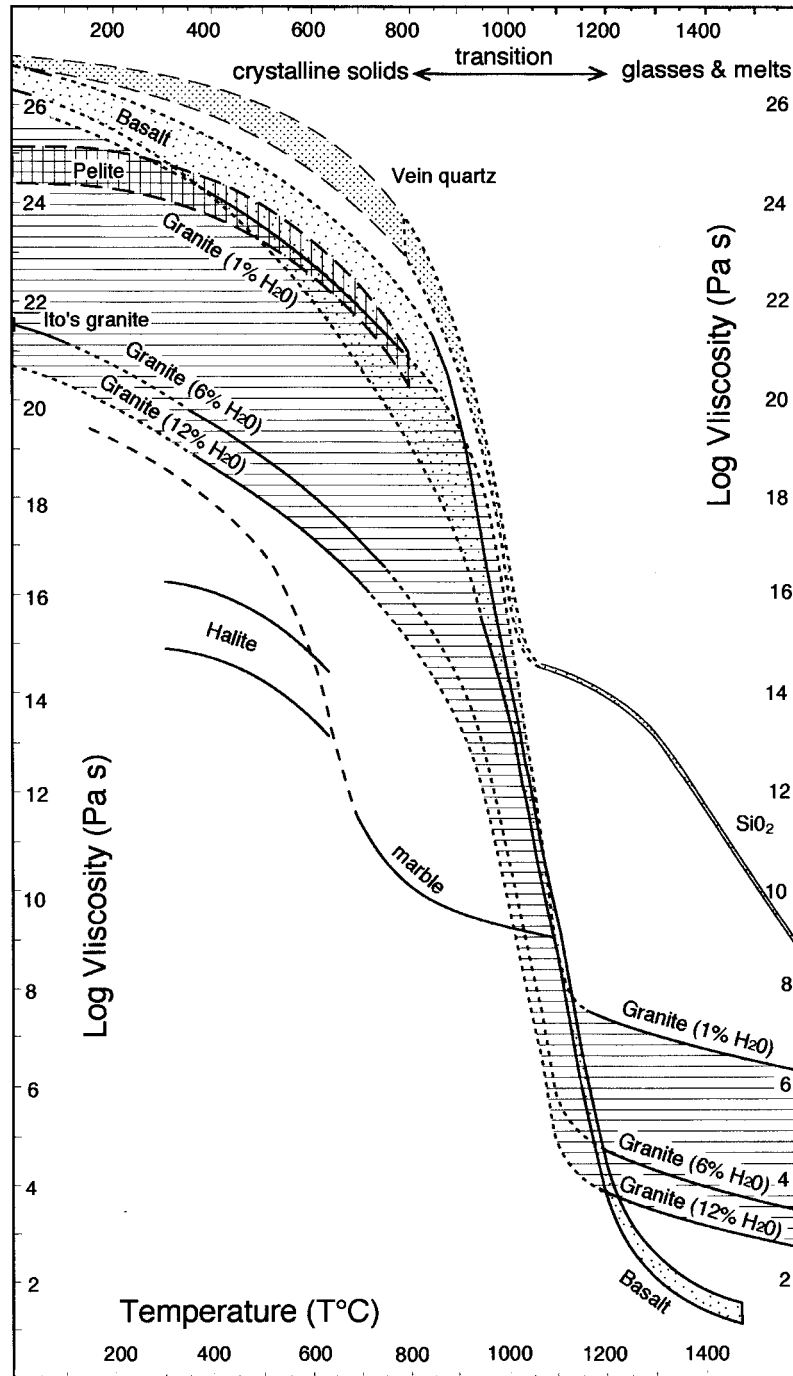


Figure 5. Viscosities for ductile crystalline rocks and their melts plotted against temperature. Solid boundaries indicate experimental data (mainly from Cruden, 1990), dashed boundaries are indicated by field data, and dotted boundaries are interpolated or extrapolated. Do you have data that could improve this diagram?

more tractable within geology departments than the link between structural geology and modelling which is often carried out by geophysicists. More likely, the opportunity has been neglected because modellers have not realised the possibility of constraining viscosity

ratios from field data and have not been demanding viscosity values. The obvious way to further subdivide rheological facies and quantify rock viscosities on the basis of structural or fabric relationships is by feed-

back between modellers who provide the tools and field geologists who provide the figures.

Acknowledgements

I thank many colleagues, past and present, for useful discussions about various aspects of this subject and remember in particular: Harro Schmeling, Dimitrios Sokoutis, Genevieve Mulugeta, Sandy Cruden, Roberto Weinberg, Bernard Schott, Sue Treagus and Neil Mancktelow. Any mistakes that remain are mine, not theirs.

References

- Biot, M.A., 1961. Theory of folding of stratified viscoelastic media and its implications in tectonics and orogenesis. *Geological Society of America Bulletin* 72, 1595–1631.
- Chapple, W.M., 1970. The finite-amplitude instability in the folding of layered rocks. *Canadian Journal of Earth Science* 7, 457–465.
- Cruden, A.C., 1990. Flow and fabric development during the diapiric rise of magma. *Journal of Geology* 98, 681–698.
- Fletcher, R.C., 1974. Wavelength selection in the folding of a single layer with power-law rheology. *American Journal of Science* 274, 1029–1043.
- Fletcher, R.C., 1977. Folding of a single viscous layer: exact infinitesimal-amplitude solution. *Tectonophysics* 39, 593–606.
- Fletcher, R.C., Sherwin, J., 1978. Arc lengths of single fold layers: a discussion of the comparison between theory and observation. *American Journal of Science* 278, 1085–1098.
- Hudleston, P.J., 1973. Fold morphology and some geometrical implications of theories of fold development shape. *Tectonophysics* 16, 1–46.
- Ito, H., 1979. Rheology of the crust based on long-term creep tests. *Tectonophysics* 52, 624–641.
- Pfiffner, O.A., Ramsay, J.G., 1982. Constraints on geological strain rates, arguments from finite strain states of naturally deformed rocks. *Journal of Geophysical Research* 87, 311–321.
- Price, N.J., 1975. Rates of deformation. *Journal of the Geological Society of London* 131, 553–575.
- Pye, K., 1994. *Sediment Transport and Depositional Processes*. Blackwell, Oxford.
- Ramsay, J.G., 1967. *Folding and Fracturing of Rocks*. McGraw-Hill, New York.
- Sherwin, J., Chapple, W.M., 1968. Wavelengths of single layer folds: a comparison between theory and observation. *American Journal of Science* 266, 167–179.
- Smith, R.B., 1975. Unified theory for the onset of folding, boudinage, and mullion structure. *Geological Society of America Bulletin* 86, 1601–1609.
- Smith, R.B., 1977. Formation of folds, boudinage, and mullions in non-Newtonian materials. *Geological Society of America Bulletin* 88, 312–320.
- Smith, R.B., 1979. The folding of a strongly non-Newtonian layer. *American Journal of Science* 279, 272–287.
- Sokolovski, W.W., 1945. The theory of plasticity—an outline of work done in Russia. *Journal of Applied Mechanics* 13, A1–A2.
- Sokoutis, D., 1987. Finite strain effects in experimental mullions. *Journal of Structural Geology* 9, 233–242.
- Sokoutis, D., 1990. Experimental mullions in single and double interfaces. *Journal of Structural Geology* 12, 365–373.
- Talbot, C.J., 1970. The minimum strain ellipsoid using deformed quartz veins. *Tectonophysics* 9, 47–76.
- Talbot, C.J., 1983. Microdiorite sheet intrusions as incompetent time and strain markers in the Moine assemblage NW of Great Glen fault. *Transactions of the Royal Society Edinburgh* 74, 137–152.
- Talbot, C.J., Sokoutis, D., 1992. The importance of incompetence. *Geology* 20, 951–953.
- Talbot, C.J., Sokoutis, D., 1995. Strain ellipsoids from incompetent dykes: application to volume loss during mylonitization in the Singö gneiss zone, central Sweden. *Journal of Structural Geology* 17, 927–984.
- Treagus, S.H., 1999. Are viscosity ratios of rocks measurable from cleavage refraction? *Journal of Structural Geology* 21, 895–901.
- Treagus, S.H., 1988. Strain refraction in layered systems. *Journal of Structural Geology* 10, 517–527.
- Treagus, S.H., 1983. A theory of finite strain variation through contrasting layers, and its bearing on cleavage refraction. *Journal of Structural Geology* 5, 351–368.
- Treagus, S.H., Sokoutis, D., 1992. Laboratory modelling of strain variations across rheological boundaries. *Journal of Structural Geology* 14, 405–424.